Microencapsulation of *Ruellia tuberosa* L. Extracts Using Alginate: Preparation, Biological Activities, and Release

Andriana Kusuma Pertiwi[1], Choirin Annisa[1], Zubaidah Ningsih[1], and Anna Safitri[1,2*]

[1]*Department of Chemistry, Faculty of Mathematics and Natural Sciences, Brawijaya University, Jl. Veteran, Malang 65145, Indonesia*

[2]*Research Centre of SMONAGENES (Smart Molecules of Natural Genetic Resources), Brawijaya University, Jl. Veteran, Malang 65145, Indonesia*

* ***Corresponding author:***

email: a.safitri@ub.ac.id

Received: August 3, 2022
Accepted: November 1, 2022

DOI: 10.22146/ijc.76821

Abstract: *The bioactive compounds naturally present in plants have great importance due to their biological characteristics. These substances could lose their active characteristics since they are highly unstable. Microencapsulation is one of the techniques to improve stability and protect these compounds. In this work,* Ruellia tuberosa *L. ethanolic extracts microcapsules were prepared using a freeze-drying method by varying pH, alginate concentration, and stirring time. The encapsulation efficiency (EE), characteristics, alpha-amylase inhibition activity, and release behavior of the microcapsules were investigated. The results highlighted that the highest encapsulation efficiency for the microcapsules was obtained at pH 6, alginate concentration of 1% (w/v), and 30 min of stirring time (51.63% EE). The microcapsules mostly had spherical shapes with a mean diameter of 197.53 µm. The alpha-amylase inhibition assay from microcapsules resulted in the IC_{50} value of 46.66 ± 0.13 µg/mL, demonstrating high biological activity. The bioactive substances from microcapsules were released during intervals of 30–120 min at pH values of 1.2 and 7.4. Only 3.51% of the bioactive substances were released at pH 1.2 after 120 min, compared to 55.78% at pH 7.4. Overall, this work confirms the possibility of developing plant extracts with preserved biological activity using the produced microcapsules.*

Keywords: *alginate; alpha-amylase; freeze drying; microencapsulation;* Ruellia tuberosa *L.*

■ INTRODUCTION

Discovering bioactive compounds in natural materials can support the expansion of their functional value in both disease prevention and treatment. Indonesia has a wide variety of plants and has been represented as one of the best producers of medicinal plants. Along with the times, the use of medicinal plants in the treatment of disease increased due to their fewer side effects [1-2]. *Ruellia tuberosa* Linn is a herbaceous plant of the *Acanthaceae* family from Central America and has widely spread in Southeast Asia countries, such as Indonesia. Based on the previous study, the leaves of this plant had anti-inflammatory activity; the roots and stems can be used as a disinfectant; the flower parts were used in the treatment of wounds [3]. This plant had also been proven to have antioxidant, anti-microbial, anti-cancer, and antidiabetic activities [4].

Several previous studies stated that the hydroethanolic extract of *R. tuberosa* L. contained several secondary metabolites compounds, such as flavonoids, phenolic compounds, ascorbic acid, and steroids [3-5]. Flavonoids can demonstrate antidiabetic activity through their function as antioxidants. The presence of hydroxyl groups (O-H) and conjugated double bonds in the structure of flavonoids produced antioxidant activity [6]. However, bioactive compounds like flavonoids are sensitive to environmental conditions such as pH or temperature and have low bioavailability

[7]. The poor bioavailability may affect the number of bioactive compounds that can attain the circulatory system. Hence, the microencapsulation method was required to protect these compounds [8]. Microencapsulation is the shielding process of small particles using a polymer. This method resulted in microcapsules with a size range of 2–2000 μm [9-10]. The primary purpose of microencapsulation is to avoid the degradation or inactivation of the active compounds due to the unstable environmental conditions [9].

Ionotropic gelation is one of the techniques in the encapsulating process based on the electrostatic interaction between two ionic species, where one of them is a polymer. The bioactive compounds from natural materials may be trapped between the polymer chains and form microcapsule beads [11-12]. A common polymer used in the microencapsulation process is sodium alginate due to its ability to form a very versatile, biocompatible, and non-toxic matrix to encapsulate the compounds [13]. Furthermore, the calcium chloride addition as a cross-linker plays a role in forming alginate beads due to the exchange of sodium ions with calcium cations. The resulting cross-linked beads were beneficial for the controlled release of bioactive molecules [14]. Drying is a necessary process to obtain microcapsules. One of the drying techniques that are generally used is freeze-drying. This technique may prevent the substances inside the dried microcapsules from degradation due to high temperatures [15-16]. Numerous factors, including pH of medium, coating material concentration, and stirring time contribute to the properties of microcapsules. Carboxylate groups in sodium alginate structure can be readily dissociated and form ionic bonds in an acid solution. The coating materials concentration and stirring time may affect the size of the microcapsules. In addition, smaller microcapsules may generate greater efficiency [17-18].

Due to the antidiabetic activity of *R. tuberosa* L. extracts, the inhibition against alpha-amylase can be conducted to determine their biological activities. Alpha-amylase is one of the targeted enzymes for type 2 diabetes mellitus (DM) treatment. The alpha-amylase enzyme (E.C.3.2.1.1) is a hydrolase class enzyme catalyzing the hydrolysis of α-1,4-glycosidic bonds of amylum to produce glucose and maltose [19]. Theoretically, inhibition of the alpha-amylase is expected to slow down the hydrolysis of carbohydrates and the formation of glucose, so this may automatically reduce the post-prandial glucose levels [20]. Moreover, the resistance of microcapsules in carrying the bioactive compound must be done through a microcapsule release test [21]. The release of microcapsules is carried out by evaluating the amount of released active compounds at very acidic (pH 1–3) and physiological conditions (pH 7.4) [22]. In this analysis, the zero-order release kinetic model is used to determine the relationship between the release time and percentage of microcapsules. The zero-order kinetic model is effectively considered for the sustained released samples [23-24].

This study was aimed to examine the process of microencapsulation using the freeze-drying technique. Calcium chloride, which serves as a cross-linker, and sodium alginate polymer constructed the shielding components. In order to find the ideal microcapsule conditions, a number of variables were examined, including pH, sodium alginate content, and stirring time. Additionally, an alpha-amylase inhibition experiment was performed on microcapsules under the optimum conditions to determine their effectiveness in treating type 2 diabetes mellitus.

■ EXPERIMENTAL SECTION

Materials

The materials were acquired from Merck: sodium alginate (≥ 99%, molecular biology grade), calcium chloride ($CaCl_2$), aluminum chloride ($AlCl_3$), alpha-amylase enzyme originated from *Aspergillus oryzae* (≥ 150 units/mg protein), D-(+) glucose (analytical standard), glacial acetic acid (pharmaceutical primary standard), soluble starch (from potato, ACS grade), sodium hydroxide (≥ 98%, pellets, anhydrous), potassium sodium tartrate tetrahydrate (≥ 99%), sodium acetate (anhydrous, ≥ 99%), 3,5-dinitrosalicylic acid (DNS) reagent (≥ 98%, HPLC grade), acarbose (≥ 95%), release mediums (simulated gastric fluid (SGF) and simulated intestinal fluid (SIF)). The *R. tuberosa* L. root

powder was purchased with a letter confirming the species from UPT Materia Medica Batu in East Java.

Instrumentation

The instrumentations used in this study were UV-Vis spectrophotometer (Shimadzu), Fourier transform infrared spectrometer (FTIR, Shimadzu Prestige 21), particle size analyzer (PSA, CILAS 1090), and scanning electron microscope (SEM, TM 3000 Hitachi).

Procedure

Preparation of R. tuberosa *L. extract*

A total of 250 g of *R. tuberosa* L. root powder was macerated using 96% ethyl alcohol for 3 × 24 h, in the volume ratio of 4:1 with the dried weight. The resulting extracts were filtrated and evaporated using a rotary evaporator (120 rpm; 50 °C) to acquire the concentrated extracts. For subsequent analysis, the concentrated extracts were stored at a low temperature of 4 °C.

Microencapsulation of R. tuberosa *L. extracts*

The 2% sodium alginate (w/v) solution was prepared in 10 mL of 1% acetate buffer (v/v, pH variations of 4, 5, 6, and 7). Then, 0.5 g extracts of *R. tuberosa* L. were dissolved with 1 mL of 96% ethyl alcohol. The mixture was gradually added to the sodium alginate solution. The mixture was stirred using a magnetic stirrer at a speed of 300 rpm until. After that, the mixture was added dropwise using a syringe to 40 mL of calcium chloride solution (0.1 M) and stirred again with a magnetic stirrer for 30 min. The forming alginate beads were washed using distilled water to remove unreacted calcium chloride ($CaCl_2$) from the surface of the beads. Then, the beads were freeze-dried for 6 h with a temperature of -55 °C and air pressure of -60 mmHg until they changed to microcapsules powder.

The same process was repeated under different conditions with the following sodium alginate concentration of 1; 1.5; 2; and 2.5% (w/v). The initial pH contributing to the optimum percentage of encapsulation efficiency was used, which was also conducted in other conditions. Lastly, the influence of stirring time was established using the same steps with different stirring times at 15, 30, 45, and 60 min. The highest percentage of encapsulation efficiency (%EE) was used to estimate the optimum conditions of microcapsules.

Encapsulation efficiency

The encapsulation efficiency expressed the percentage of encapsulated active ingredients in the polymer solution. This value denoted the effectiveness of shielding materials in trapping the extract [24]. The encapsulation efficiency was determined using the Eq. (1).

$$\text{Encapsulation efficiency}(\%) = \frac{\text{Total flavonoid content in microcapsules}}{\text{Total flavonoid content in extracts}} \times 100\% \quad (1)$$

The colorimetric technique with aluminum chloride reagent was used to determine the total flavonoid content in samples. The extract and microcapsule of *R. tuberosa* L. were prepared by dissolving 5 mg samples in 3 mL methanol, incubating at 40 °C for 45 min, and centrifuging at 1,000 rpm for 2 min. An amount of 0.6 mL of prepared solution was combined with 0.6 mL of 2% of $AlCl_3$. The combined solution was then incubated for 23 min at room temperature. UV-Vis spectrophotometer was used to measure the absorbance of solution at a wavelength of 420 nm. According to the quercetin standard curve plot ($y = 0.0469x + 0.0138$, $R^2 = 0.9977$), the amount of total flavonoid content in each sample was determined and reported as mg quercetin equivalent (QE)/g. All the determinations were completed in triplicate.

Alpha-amylase inhibition assay

All samples, including extracts and microcapsules of *R. tuberosa* L., and the positive control acarbose, were made in numerous concentrations (20–100 µg/mL). Then, 250 µL of each sample was added to 250 µL alpha-amylase enzyme solution (10 U/mL), which was then incubated for 30 min at 37 °C. The mixture was then mixed with 250 µL of 1% soluble starch solution (w/v) and incubated at 25 °C for 10 min. Furthermore, 500 µL of DNS reagent was included, and the entire mixture was heated to a temperature of boiling water and incubated for 5 min until the color changed into reddish brown. The solution was then mixed with 5 mL of distilled water after the solution had been cooled down under running

water. Lastly, a UV-Vis spectrophotometer operating at a wavelength of 480 nm was used to test the absorbance of solution. The assays were carried out in triplicates. Eq. (2) was used to determine the alpha-amylase inhibitory activity:

$$\text{Percentage of enzyme inhibition (\%)} = \frac{\text{Absorbance of control} - \text{Absorbance of sample}}{\text{Absorbance of control}} \times 100\% \quad (2)$$

The results were represented by the IC_{50} value, which can be defined as the level of inhibition needed to block 50% of the activity of the alpha-amylase enzyme. Plotting a linear regression equation between sample concentration and enzyme percent inhibition was carried out to determine the IC_{50} value.

In vitro *release study*

The *in vitro* release of extracts from microcapsules matrix was performed in the release medium consisting of simulated gastric fluid (SGF) and simulated intestinal fluid (SIF) with pH of 1.2 and 7.4, respectively. The release medium was prepared, and the microcapsules were added. Next, the mixture was constantly stirred at 100 rpm and placed in the water bath at 37 °C. A total of 10 mL of the solution was sampled at the intervals of 30, 60, 90, and 120 min, and then analyzed using a UV-Vis spectrophotometer at the wavelength of 420 nm. By using the quercetin standard curve, the concentration of the substance released from the microcapsules was determined as a total flavonoid content. Eq. (3) was used to express the outcome as a percentage of release (%).

$$\text{Percentage of release \%)} = \frac{\text{Total flavonoid content release from microcapsules}}{\text{Total flavonoid content of microcapsules in optimum condition}} \times 100\% \quad (3)$$

FTIR, particle size distribution, and SEM analyses

A dried sample that had been compressed into a KBr pellet was used for the FTIR measurement, which was conducted in the 4000–400 cm^{-1} wavenumber region using an FTIR Shimadzu Type IR Prestige-21. A CILAS 1090 PSA was used to analyze the distribution and size of microcapsules. An SEM TM 3000 Hitachi was used to examine the microcapsule's surface morphology and form at magnifications ranging from 4,000× to 12,000×.

Data analysis

The mean ± standard deviation was used to express the results. A software, Statistical Package for The Social Science (SPSS) v.26, was used to conduct the statistical analysis. The one-way analysis of variance (ANOVA) and Tukey's HSD test was then used to assess the true difference from each variation. The differences were deemed statistically significant at $p < 0.05$.

■ RESULTS AND DISCUSSION

The dried microcapsules from *R. tuberosa* L. extracts were prepared using the freeze-drying technique. The optimization was carried out to determine the best conditions leading to the formation of microcapsules with a high percentage of encapsulation efficiency. Table 1–3 expresses the percentage of encapsulation efficiency from microcapsules set up at diverse pH, sodium alginate concentrations, and stirring times. The highest encapsulation efficiency has resulted in *R. tuberosa* L.

Table 1. Effect of pH on the encapsulation efficiency of *R. tuberosa* L.

pH*	Encapsulation efficiency (%)**
4	33.72 ± 0.26[b]
5	41.73 ± 0.25[c]
6	46.21 ± 0.32[d]
7	30.56 ± 0.24[a]

*Microcapsules were prepared using 2% (w/v) of sodium alginates for 30 min stirring time; **Different notations, using the One-Way ANOVA test with a level of confidence α = 5%, indicate significant differences between conditions

Table 2. Effect of sodium alginate concentration on the encapsulation efficiency of *R. tuberosa* L.

Concentration of sodium alginate (%w/v)*	Encapsulation efficiency (%)**
1	51.53 ± 0.15[d]
1.5	44.93 ± 0.18[c]
2	37.84 ± 0.12[b]
2.5	32.46 ± 0.26[a]

*Microcapsules were prepared at optimum pH 6 for 30 min stirring time; **Different notations, using the One-Way ANOVA test with a level of confidence α = 5%, indicate significant differences between conditions

Table 3. Effect of stirring time on the encapsulation efficiency of *R. tuberosa* L.

Stirring time (min)*	Encapsulation efficiency (%)**
15	50.92 ± 0.15^{c}
30	51.63 ± 0.09^{d}
45	49.79 ± 0.09^{b}
60	42.17 ± 0.2^{a}

*Microcapsules were prepared at optimum pH 6 using the optimum concentration of sodium alginate of 1% (w/v); **Different notations, using the One-Way ANOVA test with a level of confidence α = 5%, indicate significant differences between conditions

microcapsules set in pH 6, 1% (w/v) sodium alginate, and 30 min stirring time, with 51.63% encapsulation efficiency.

The microcapsules prepared at pH 6 showed the highest encapsulation efficiency. Sodium alginate can dissolve in acidic pH due to the p*K*a values of mannuronic and guluronic acid residues around 3.38–3.65 [25]. Moreover, in acidic solutions, the repulsion force among groups in sodium alginate decreased, so the gel strength tended to increase [26]. At weaker acidic pH (~6), sodium alginate dissociates easier and breaks the bond between the sodium (Na^+) ion and carboxylate ion (COO^-) of mannuronic or guluronic acid. As a result, the divalent ion Ca^{2+} of cross-linker $CaCl_2$ displaces Na^+ ions and forms ionic bonds with carboxylate ions. Thus, the increasing ionic bonds might strengthen the matrix, escalate the amount of encapsulated bioactive ingredients, and result in the greatest encapsulation efficiency [26-27]. The results agreed with previous research [28], which stated that a higher pH solution would produce less protonated forms. The protonation of the carboxylate anions can interrupt the coordination with calcium cations and reduce the existing sites for cross-linking.

In this research, the optimum condition of microcapsules was acquired at a sodium alginate concentration of 1% (w/v). The higher sodium alginate concentration produced a lower encapsulation efficiency, as shown in Table 2. Similar results were informed by Wibowo et al. [29], in which encapsulation efficiency decreased with the enhancement of sodium alginate concentration. A lower concentration of sodium alginate generated a larger pore size of the beads. In contrast, the pore size of the beads decreased with the increase in sodium alginate concentration. Therefore, enhancing sodium alginate concentration might inhibit the entrance of bioactive compounds into the beads and lead to lower encapsulation efficiency.

The stirring time was also a parameter investigated in this study. The short stirring time resulted in particle aggregates and less discreet microcapsules, whereas the longer time resulted in particles with fragile and breakable properties [30-31]. Table 3 shows that the stirring time of 30 min gave the maximum encapsulation efficiency. This results were similar to earlier research [30], which explained that smaller microcapsules formed at a stirring time of 30 min with the increased size distribution. As a result, the larger particle surface area was developed and facilitated the adsorption of extracts into the polymer matrix.

The antidiabetic activity of a sample can be determined by an alpha-amylase inhibition assay. The samples used in this assay were the ethanolic extract of *R. tuberosa* L., microcapsules prepared under the optimum conditions, and acarbose. Based on Table 4, all samples displayed a high alpha-amylase enzyme inhibition, as seen from the low IC_{50} values. The microcapsules had a higher IC_{50} value (46.66 ± 0.13 μg/mL) than *R. tuberosa* L. ethanolic extract (33.77 ± 0.87 μg/mL). A higher IC_{50} value corresponds to weaker inhibition activity against the

Table 4. The IC_{50} value of *R. tuberosa* L. ethanolic extracts, microcapsules, and acarbose on alpha-amylase inhibition assay

Sample	IC_{50} values (μg/mL)*
R. tuberosa L. ethanolic extract	33.77 ± 0.87^{b}
Microcapsules prepared at the optimum conditions	46.66 ± 0.13^{c}
Acarbose	24.31 ± 0.40^{a}

*Different notations, using the One-Way ANOVA test with a level of confidence α = 5%, indicate significant differences between conditions

alpha-amylase enzyme. In the microcapsule sample, the bioactive compounds cannot be entirely released. Some compounds were still restrained in a polymer matrix, resulting in a lower ability to inhibit enzyme activity [32]. The fundamental goal of microencapsulation is not to increase the antidiabetic activity of the sample but to enhance the protection and avoid the degradation of bioactive ingredients. Besides, the encapsulating samples can manage the release of bioactive compounds [33]. Hence, the microcapsule of *R. tuberosa* L. extracts had the potential role of an antidiabetic source due to the presence of flavonoid compounds [11]. Flavonoids can form a covalent bond with the alpha-amylase enzyme and change their activity due to the capability to establish quinones or lactones that react with nucleophilic groups on the enzyme [34].

Acarbose, as a positive control, had the lowest IC_{50} value of 24.31 ± 0.40 μg/mL, which denoted the most vigorous inhibitory activity against the alpha-amylase. Acarbose is a synthetic drug for DM type 2 treatment. This drug has a similar structure to oligosaccharides and acts as a competitive inhibitor of the alpha-amylase [35]. According to [34], acarbose produced maximum inhibition against alpha-amylase by suspending the digestion of carbohydrates and delaying glucose absorption. Moreover, although the ethanolic extract of *R. tuberosa* L. contains various bioactive compounds [3-5], not all of these compounds could inhibit alpha-amylase [36].

Among all the *in vitro* assays for microparticles, the release study is one of the essential parameters. Through this assay, the assessment of the safety, efficiency, and quality of the microcapsules can be found [37]. In this study, the microcapsules were dissolved in two mediums, SGF at pH 1.2 and SIF at pH 7.4. The dissolution was carried out continuously in different time variations [38].

The whole drug release process was affected by both the physical and mechanical properties of the gel shielding around the microcapsules [39]. Based on the release profile in Fig. 1, the release of microcapsules at pH 1.2 was lower than that at pH 7.4. At pH 1.2, the curve gradually increased at a 30–90 min of release time with a release value of around 1.1 to 3.2%, but then it reached a plateau of about 3.2 to 3.5% in the remaining time. The sodium alginate comprises mannuronic and guluronic acid with p*K*a values of 3.38 and 3.65, respectively. An intermolecular hydrogen bonding system could stabilize alginate beads in the medium with a pH below these p*K*a values. As a consequence, the swelling ratio of the alginate particles reduces in the gastric environment, so the encapsulated drug will be difficult to reach out from the network [25,40].

The low-release profile of microcapsules in pH 1.2 is also proven by the SEM image in Fig. 2(c). The image of released microcapsules in an acidic medium produced ruptured and folded spherical shapes. The shapes indicating that the coating matrix experienced erosion, and the microcapsules were partially bursting, resulting in a low percentage of drug release [41].

In contrast, at pH 7.4, the release value significantly increased and reached the maximum value of 55.8% at 120 min. This was due to the increase of negatively charged of carboxylate ions because of a higher level of

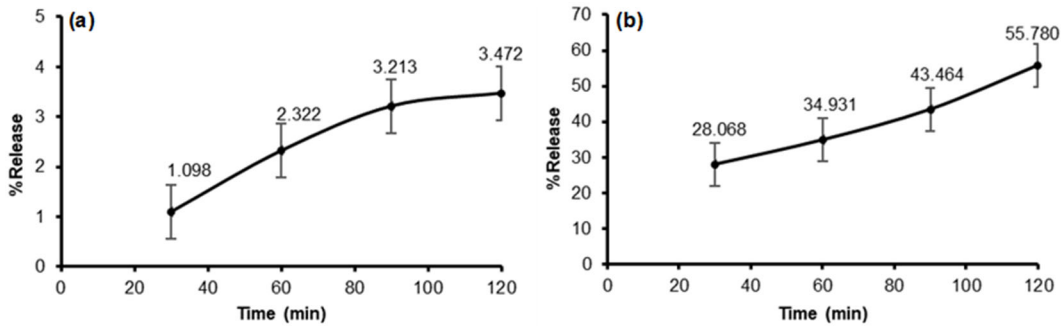

Fig 1. The released profile of microcapsules of *R. tuberosa* L. extract prepared in pH 6, 1% (w/v) sodium alginate, and 30 min stirring time at: (a) pH 1.2; (b) 7.4

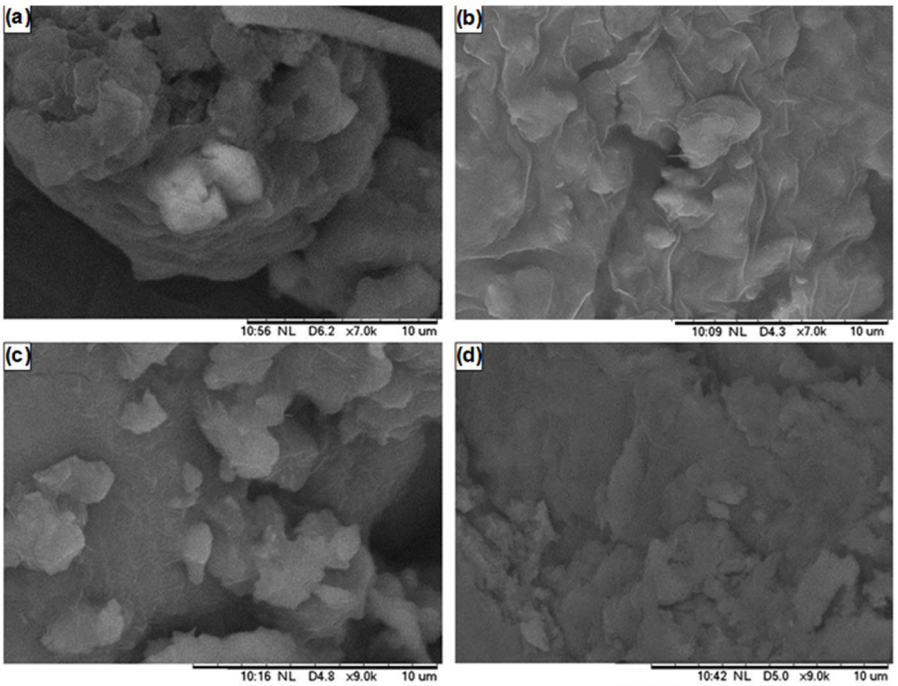

Fig 2. The SEM images of (a) *R. tuberosa* L. ethanolic extract; (b) microcapsules of *R. tuberosa* L. prepared in pH 6, 1% (m/v) sodium alginate concentration, and 30 min stirring time; (c) microcapsules released in pH 1.2; (d) microcapsules released in pH 7.4. The magnifications were 7,000× for (a) and (b), and 9,000× for (c) and (d)

ionization. These carboxylate ions might repel each other and cause the disaggregating of the alginate-$CaCl_2$ matrix structure, then lead to swollen microcapsules [42]. This result was also supported by the SEM image in Fig. 2(d) showing a flatter morphological surface than the previous one. The more released compounds might increase the intensity of matrix erosion, and the microcapsules might break more easily. The similar results have also been informed that bioactive ingredients were released more easily in the alkaline condition than in acidic pH [25].

Characterization with SEM was carried out to confirm the surface morphology of the samples. According to Fig. 2(a-b), there were difference between SEM images of extracts and microcapsules. The microcapsules showed an irregular shape with a few spherical, followed by the uniform distribution of wrinkled surfaces. This result was in agreement with a previous study that reported freeze-dried samples did not have a specific shape [43]. The irregularities of the surface and the existence of wrinkles might be allied with the low drying temperatures. The forming ice crystals during the freeze-drying step also established the cavities [43-44].

The FTIR analysis identified functional groups in *R. tuberosa* L. extracts and microcapsules. Fig. 3 shows the FTIR spectra, while the assignments of the absorption functional groups are listed in Table 5. Based on Fig. 3(a), the extract of *R. tuberosa* L. denoted the stretching vibrations of the hydroxyl (O-H) group at 3354 cm^{-1}. Then, the characteristic peaks of methine C-H stretching were observed at 2926 and 2855 cm^{-1}. Moreover, the absorption at 1608 cm^{-1} was interpreted as ketone C=O stretching, whereas peaks at 1450 and 1168 cm^{-1} showed the stretching vibrations of aromatic C=C and vinyl ether C-O-C, respectively [45]. These absorptions suggested that *R. tuberosa* L. contained flavonoid compounds [46-47].

The FTIR spectra of microcapsules of *R. tuberosa* L. (Fig. 3(b)) showed broader and higher intensity band at 3448 cm^{-1}coming the stretching vibrations of the O-H group. This peak corresponded to the sum of the peaks from coating materials, namely sodium alginate and $CaCl_2$ [48]. Then, the same absorption from the vibration of C-H methine, C=O ketone, C=C aromatic, and C-O-C vinyl ether groups also resulted in peaks 2–6 [45]. In addition,

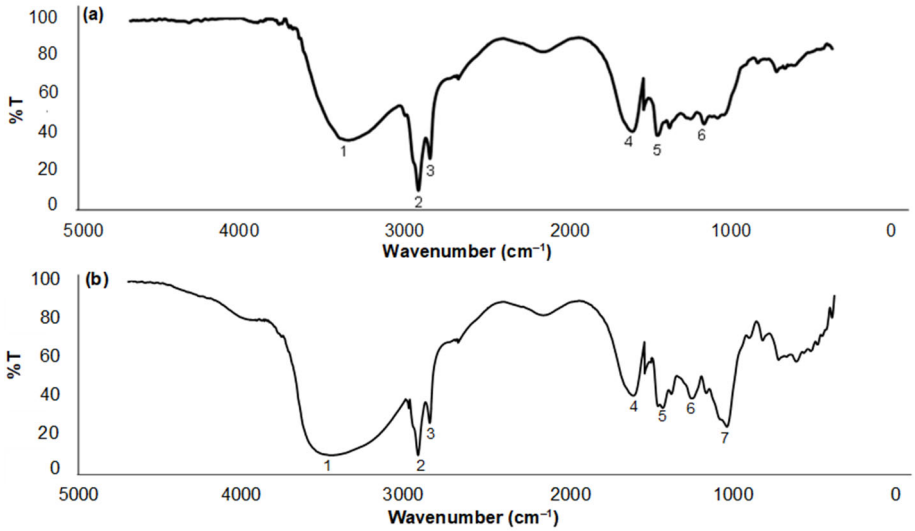

Fig 3. FTIR spectra of (a) *R. tuberosa* L. extract; (b) microcapsules of *R. tuberosa* L. extracts prepared in pH 6, 1% (w/v) sodium alginate, and 30 min stirring time

Table 5. Assignment of FTIR spectra

Peak number	Wavelength (cm^{-1})		Functional groups
	R. tuberosa L. extracts [43-45]	Microcapsules of *R. tuberosa* L. extracts [43-46]	
1	3354	3448	O-H alcohol
2	2926	2925	C-H methine
3	2855	2853	C-H methine
4	1608	1609	C=O ketone
5	1450	1429	C=C aromatic
6	1168	1252	C-O-C vinyl ether
7		1036	C-O-C aliphatic ether

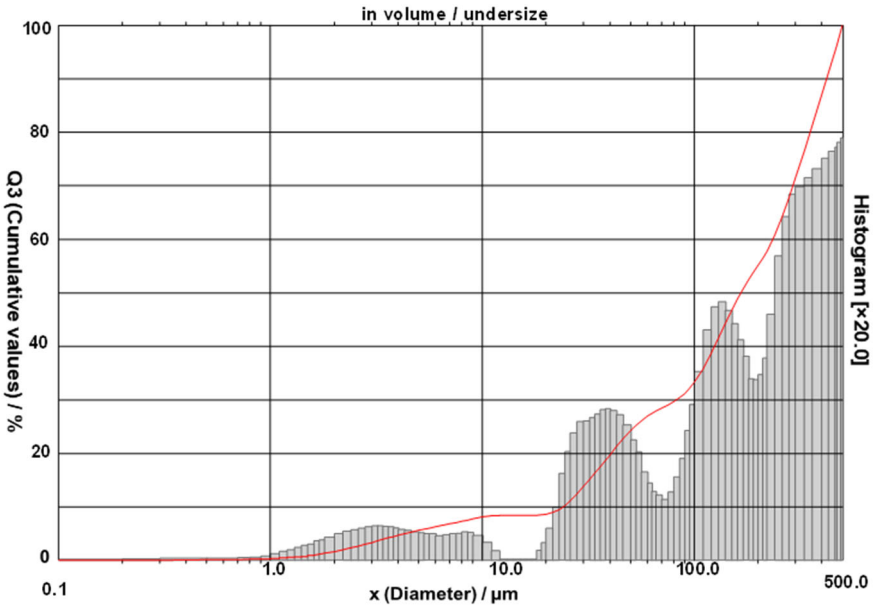

Fig 4. Particle size distribution from microcapsules of *R. tuberosa* L. extracts set in pH 6, 1% (w/v) sodium alginate, and 30 min stirring time. The mean diameter was 197.53 µm

the new absorption (peak 7) at 1036 cm^{-1}represented the presence of C-O-C aliphatic ether coming from sodium alginate [48].

In this work, the size of the microcapsules was also evaluated. The properties of powder samples majorly depend on the sizes of the particles. The PSA is the standard instrument in the sizing test. This instrument was objected to determine particle size and hydrodynamic diameter of the microcapsules [49]. The microcapsules formed in this study had a mean diameter of 197.53 m, which was in the range of microparticle size, as shown in Fig. 4. This outcome satisfied the criteria for extrusion and freeze-drying-produced particles with a size range of 15–3500 m. Extrusion is a technique that relies on the interaction of a multivalent ion with a polysaccharide gel [50-51].

■ CONCLUSION

This study has carried out the microencapsulation of *R. tuberosa* L. extracts using the freeze-drying method with sodium alginate and $CaCl_2$ as shielding materials. The optimum conditions of microcapsules were pH 6, sodium alginate concentration of 1% (w/v), and 30 min of stirring time. The alpha-amylase was inhibited by the microcapsules with an IC_{50} value of 46.66 ± 0.13 µg/mL. The *in vitro* release assay presented that the microcapsule of *R. tuberosa* L. extract was released more readily at pH 7.4 than at pH 1.2. The morphological surface analysis by SEM indicated an irregular shape with a few spherical followed by the uniform distribution of wrinkling; hence the PSA result stated that the microcapsules had micro-sized particles with a mean diameter of 197.53 µm. Moreover, the FTIR analysis demonstrated that the cross-linking between sodium alginate and $CaCl_2$ has been obtained. Microencapsulation of plant extracts can be one of the strategies for natural product enhancement with preserved biological functions.

■ ACKNOWLEDGMENTS

This work was supported by *Hibah Penelitian Doktor* grant, contract number 3110.1/UN10.F09/PN/2022, and was part of *Penelitian Tesis Magister* grant, year of 2022.

■ AUTHOR CONTRIBUTIONS

Andriana Kusuma Pertiwi conducted the experiment, Choirin Annisa analyzed the data, Andriana Kusuma Pertiwi, Anna Safitri, and Zubaidah Ningsih wrote and revised the manuscript. All authors agreed to the final version of this manuscript.

■ REFERENCES

[1] Sholikhah, E.N., 2016, Indonesian medicinal plants as sources of secondary metabolites for pharmaceutical industry, *JMedSci*, 48 (4), 226–239.

[2] Batubara, I., and Prastya, M.E., 2020, Potential use of Indonesian medicinal plants for cosmetic and oral health: A review, *J. Kim. Valensi*, 6 (1), 118–132.

[3] Khan, I., Jan, S., Shinwari, Z.K., Ali, M., Khan, Y., and Kumar, T., 2017, Ethnobotany and medicinal uses of folklore medicinal plants belonging to family acanthaceae: An updated review, *MOJ Biol. Med.*, 1 (2), 34–38.

[4] Ramadhan, M., Sabarudin, A., and Safitri, A., 2019, *In vitro* anti-microbial activity of hydroethanolic extracts of *Ruellia tuberosa* L.: Eco-friendly based-product against selected pathogenic bacteria, *IOP Conf. Ser.: Earth Environ. Sci.*, 239, 012028.

[5] Safitri, A., Roosdiana, A., Rosyada, I., Evindasari, C.A., Muzayyana, Z., and Rachmawanti, R., 2019, Phytochemicals screening and anti-oxidant activity of hydroethanolic extracts of *Ruellia tuberosa* L, *IOP Conf. Ser.: Mater. Sci. Eng.*, 509, 012017.

[6] Roosdiana, A., Permata, F.S., Fitriani, R.I., Umam, K., and Safitri A., 2020, *Ruellia tuberosa* L. extract improves histopathology and lowers malondialdehyde levels and TNF alpha expression in the kidney of streptozotocin-induced diabetic rats, *Vet. Med. Int.*, 2020, 8812758.

[7] Lucas, J., Ralaivao, M., Estevinho, B.N., and Rocha, F., 2020, A new approach for the microencapsulation of curcumin by a spray drying method, in order to value food products, *Powder Technol.*, 362, 428–435.

[8] Rahayu, I., Zainuddin, A., and Hendrana, S., 2020, Improved maleic anhydride grafting to linear low

density polyethylene by microencapsulation method, *Indones. J. Chem*., 20 (5), 1110–1118.

[9] Safitri, A., Roosdiana, A., Kurnianingsih, N., Fatchiyah, F., Mayasari, E., and Rachmawati, R., 2022, Microencapsulation of *Ruellia tuberosa* L. aqueous root extracts using chitosan-sodium tripolyphosphate and their *in vitro* biological activities, *Scientifica*, 2022, 9522463.

[10] Chaemsawang, W., Prasongchean, W., Papadopoulos, K.I., Sukrong, S., Kao, W.J., and Wattanaarsakit, P., 2018, Emulsion cross-linking technique for human fibroblast encapsulation, *Int. J. Biomater.*, 2018, 9317878.

[11] Pedroso-Santana, S., and Fleitas-Salazar, N., 2020, Ionotropic gelation method in the synthesis of nanoparticles/microparticles for biomedical purposes, *Polym. Int.*, 69 (5), 443–447.

[12] He, L., Shang, Z., Liu, H., and Yuan, Z.X., 2020, Alginate-based platforms for cancer-targeted drug delivery, *Biomed Res. Int.*, 2020, 1487259.

[13] Alvarez-Berrios, M.P., Aponte-Reyes, L.M., Diaz-Figueroa, L., Vivero-Escoto, J., Johnston, A., and Sanchez-Rodriguez, D., 2020, Preparation and *in vitro* evaluation of alginate microparticles containing amphotericin B for the treatment of *Candida* infections, *Int. J. Biomater.,* 2020, 2514387.

[14] Abasalizadeh, F., Moghaddam, S.V., Alizadeh, E., Akbari, E., Kashani, E., Fazljou, S.M.B., Torbati, M., and Akbarzadeh, A., 2020, Alginate-based hydrogels as drug delivery vehicles in cancer treatment and their applications in wound dressing and 3D bioprinting, *J. Biol. Eng.*, 14 (1), 8.

[15] Pudziuvelyte, L., Marksa, M., Sosnowska, K., Winnicka, K., Morkuniene, R., and Bernatoniene, J., 2020, Freeze-drying technique for microencapsulation of *Elsholtzia ciliata* ethanolic extract using different coating materials, *Molecules*, 25 (9), 2237.

[16] Zhao, L., Duan, X., Cao, W., Ren, X., Ren, G., Liu, P., and Chen, J., 2021, Effects of different drying methods on the characterization, dissolution rate and antioxidant activity of ursolic acid-loaded chitosan nanoparticles, *Foods*, 10 (10), 2470.

[17] Cáceres, L.M., Velasco, G.A., Dagnino, E.P., and Chamorro, E.R., 2020, Microencapsulation of grapefruit oil with sodium alginate by gelation and ionic extrusion: Optimization and modeling of crosslinking and study of controlled release kinetics, *Rev. Tecnol. Cienc.*, 39, 41–61.

[18] Bennacef, C., Desobry-Banon, S., Probst, L., and Desobry, S., 2021, Advances on alginate use for spherification to encapsulate biomolecules, *Food Hydrocolloids*, 118, 106782.

[19] Farooq, M.A., Ali, S., Hassan, A., Tahir, H.M., Mumtaz, S., and Muntaz, S., 2021, Biosynthesis and industrial applications of α-amylase: A review, *Arch. Microbiol.*, 203 (4), 1281–1292.

[20] Mphahlele, M.J., Agbo, E.N., and Choong, Y.S., 2021, Synthesis, structure, carbohydrate enzyme inhibition, antioxidant activity, in silico drug-receptor interactions and drug-like profiling of the 5-styryl-2-aminochalcone hybrids, *Molecules*, 26 (9), 2692.

[21] Parhizkar, A., and Asgary, S., 2021, Local drug delivery systems for vital pulp therapy: A new hope, *Int. J. Biomater.*, 2021, 5584268.

[22] Braim, S., Śpiewak, K., Brindell, M., Heeg, D., Alexander, C., and Monaghan, T., 2019, Lactoferrin-loaded alginate microparticles to target *Clostridioides difficile* infection, *J. Pharm. Sci.*, 108 (7), 2438–2446.

[23] Fauzi, M.A.R.D., Hendradi, E., Pudjiastuti, P., and Widodo, R.T., 2021, Analysis of dissolution of salicylamide from carrageenan based hard-shell capsules: A study of the drug-matrix interaction, *Indones. J. Chem.*, 21 (1), 148–156.

[24] Witzler, M., Vermeeren, S., Kolevatov, R.O., Haddad, R., Gericke, M., Heinze, T., and Schulze, M., 2021, Evaluating release kinetics from alginate beads coated with polyelectrolyte layers for sustained drug delivery, *ACS Appl. Bio Mater.*, 4 (9), 6719–6731.

[25] Chuang, J.J., Huang, Y.Y., Lo, S.H., Hsu, T.F., Huang, W.Y., Huang, S.L., and Lin, Y.S., 2017, Effects of pH on the shape of alginate particles and its release behavior, *Int. J. Polym. Sci.*, 2017, 3902704.

[26] Ramdhan, T., Ching, S.H., Prakash, S., and Bhandari, B., 2019, Time dependent gelling properties of cuboid alginate gels made by external gelation method: Effects of alginate-$CaCl_2$ solution ratios and pH, *Food Hydrocolloids*, 90, 232–240.

[27] Perkasa, D.P., Erizal, E., Purwanti, T., and Tontowi, A.E., 2018, Characterization of semi-interpenetrated network alginate/gelatin wound dressing crosslinked at Sol Phase, *Indones. J. Chem.*, 18 (2), 367–375.

[28] dos Santos de Macedo, B., de Almeida, T., da Costa Cruz, R., Netto, A.D.P., da Silva, L., Berret, J.F., and Vitorazi, L., 2020, Effect of pH on the complex coacervation and on the formation of layers of sodium alginate and PDADMAC, *Langmuir*, 36 (10), 2510–2523.

[29] Wibowo, A.A., Suryandari, A.S., Naryono, E., Pratiwi, V.M., Suharto, M., and Adiba, N., 2021, Encapsulation of clove oil within Ca-alginate-gelatine complex: Effect of process variables on encapsulation efficiency, *JTKL*, 5 (1), 71–77.

[30] Ningsih, Z., Lestari, M.L.A.D., and Maharin, S.A.R., 2021, Preparation and characterization of curcumin nanoemulsion in olive oil-tween 80 system using wet ball milling method, *ICS Phys. Chem.*, 1 (1), 16–19.

[31] Panigrahi, D., Sahu, P.K., Swain, S., and Verma, R.K., 2021, Quality by design prospects of pharmaceuticals application of double emulsion method for PLGA loaded nanoparticles, *SN Appl. Sci.*, 3 (6), 638.

[32] Safitri, A., Roosdiana, A., Hitdatania, E., and Damayanti, S.A., 2022, *In vitro* alpha-amylase inhibitory activity of microencapsulated *Cosmos caudatus* Kunth extracts, *Indones. J. Chem.*, 22 (1), 212–222.

[33] Suratman, A., Purwaningsih, D.R., Kunarti, E.S., and Kuncaka, A., 2020, Controlled release fertilizer encapsulated by glutaraldehyde-crosslinked chitosan using freeze-drying method, *Indones. J. Chem.*, 20 (6), 1414–1421.

[34] Oyedemi, S.O., Oyedemi, B.O., Ijeh, I.I., Ohanyerem, P.E., Coopoosamy, R.M., and Aiyegoro, O.A., 2017, Alpha-amylase inhibition and antioxidative capacity of some antidiabetic plants used by the traditional healers in southeastern Nigeria, *Sci. World J.*, 2017, 3592491.

[35] Hsu, P.F., Sung, S.H., Cheng, H.M., Shin, S.J., Lin, K.D., Chong, K., Yen, F.S., Yu, B.H., Huang, C.T., and Hsu, C.C., 2018, Cardiovascular benefits of acarbose vs sulfonylureas in patients with type 2 diabetes treated with metformin, *J. Clin. Endocrinol. Metab.*, 103 (10), 3611–3619.

[36] Chelladurai, G.R.M., and Chinnachamy, C., 2018, Alpha amylase and alpha glucosidase inhibitory effects of aqueous stem extract of *Salacia oblonga* and its GC-MS analysis, *Braz. J. Pharm. Sci.*, 54 (1), e17151.

[37] Weng, J., Tong, H.H.Y., and Chow, S.F., 2020, *In vitro* release study of the polymeric drug nanoparticles: Development and validation of a novel method, *Pharmaceutics*, 12 (8), 732.

[38] Li, L., Li, J., Si, S., Wang, L., Shi, C., Sun, Y., Liang, Z., and Mao, S., 2015, Effect of formulation variables on *in vitro* release of a water-soluble drug from chitosan–sodium alginate matrix tablets, *Asian J. Pharm. Sci.*, 10 (4), 314–321.

[39] Abbasnezhad, N., Zirak, N., Shirinbayan, M., Tcharkhtchi, A., and Bakir, F., 2021, On the importance of physical and mechanical properties of PLGA films during drug release, *J. Drug Delivery Sci. Technol.*, 63, 102446.

[40] Sreekanth Reddy, O., Subha, M.C.S., Jithendra, T., Madhavi, C., and Chowdoji Rao, K., 2021, Curcumin encapsulated dual cross linked sodium alginate/montmorillonite polymeric composite beads for controlled drug delivery, *J. Pharm. Anal.*, 11 (2), 191–199.

[41] Lengyel, M., Kállai-Szabó, N., Antal, V., Laki, A.J., and Antal, I., 2019, Microparticles, microspheres, and microcapsules for advanced drug delivery, *Sci. Pharm.*, 87 (3), 20.

[42] Thomas, D., Latha, M.S., and Kurienthomas, K., 2018, Zinc-alginate beads for the controlled release of rifampicin, *Orient. J. Chem.*, 34 (1), 428–433.

[43] Moayyedi, M., Eskandari, M.H., Rad, A., Ziaee, E., and Khodaparast, M., 2018, Effect of drying methods (electrospraying, freeze drying and spray drying) on survival and viability of microencapsulated

Lactobacillus rhamnosus ATCC 7469, *J. Funct. Foods*, 40, 391–399.

[44] Makouie, S., Alizadeh, M., Maleki, O., and Khosrowshahi, A., 2019, Optimization of wall components for encapsulation of *Nigella sativa* seed oil by freeze-drying, *IFSTJ*, 3 (1), 1–9.

[45] Nandiyanto, A.B.D., Oktiani, R., and Ragadhita, R., 2019, How to read and interpret FTIR spectroscope of organic material, *IJoST*, 4 (1), 97–118.

[46] Abbas, O., Compère, G., Larondelle, Y., Pompeu, D., Rogez, H., and Baeten, V., 2017, Phenolic compound explorer: A mid-infrared spectroscopy database, *Vib. Spectrosc.*, 92, 111–118.

[47] Kartini, K., Putri, L.A.D., and Hadiyat, M.A., 2020, FTIR-based fingerprinting and discriminant analysis of *Apium graveolens* from different locations, *J. Appl. Pharm. Sci.*, 10 (12), 62–67.

[48] Nastaj, J., Przewłocka, A., and Rajkowska-Myśliwiec, M., 2016, Biosorption of Ni(II), Pb(II) and Zn(II) on calcium alginate beads: Equilibrium, kinetic and mechanism studies, *Polish J. Chem. Technol.*, 18 (3), 81–87.

[49] Gerasimov, A.M., Eremina, O.V., Cherkasova, M.V., and Dmitriev, S.V., 2021, Application of particle-size analysis in various industries, *J. Phys.: Conf. Ser.*, 1728, 012003.

[50] Pech-Canul, Á.C., Ortega, D., García-Triana, A., González-Silva, N., and Solis-Oviedo, R.L., 2020, A brief review of edible coating materials for the micro encapsulation of probiotics, *Coatings*, 10 (3), 197.

[51] de Freitas Santos, P.D., Rubio, F.T.B., da Silva, M.P., Pinho, L.S., and Favaro-Trindade, C.S., 2021, Microencapsulation of carotenoid-rich materials: A review, *Food Res. Int.*, 147, 110571.